CHAPTER III
SILANE MODIFIED STARCH FOR COMPATIBLE REACTIVE BLEND WITH POLY(LACTIC ACID)

3.1 Abstract

A reactive blend of poly(lactic acid) (PLA) and a surface modified starch by silane coupling agent to achieve compatibility is proposed. A detailed structural analysis by using ^{1}H-^{1}H TOCSY NMR spectrum clarifies, for the first time, that chloropropyl trimethoxysilane (CPMS) forms covalent bonds with starch during starch modification and consequently forms covalent bonds with PLA in the step of blending to produce a reactive blend of PLA and CP-starch. The CP-starch covalently bound with PLA provides the compatibility between PLA and starch and also plays the role as nucleating agent as identified from a significant increase of degree of crystallinity (as high as 10-15 times), as well as induces chain mobility, as identified from a slight decrease in glass transition temperature (~5-10 °C). The PLA/CP-starch film performed as well as neat PLA with slight increases in tensile strength and elongation at break, as compared to other PLA/silane modified starch films.

Keywords: poly(lactic acid), starch, compatibility, silane coupling agent, reactive blend

3.2 Introduction

PLA is a biodegradable plastic derived from 2-hydroxy propionic acid which is comparable to commodity thermoplastics in terms of high transparency, moderate gas permeability, and high strength. Nevertheless, PLA has limitations regarding price and brittleness. The points to develop PLA, therefore, are mostly related to the cost reduction and the mechanical properties improvement (Garlotta, 2002; Huneault & Li, 2007).

The key to improve the mechanical properties is to initiate a good balance between the crystalline and amorphous phases of PLA. Up to the present, ways to

accelerate crystallization, especially the addition of nucleating agent, have been proposed. The nucleating agent plays an important role in reducing the surface free energy barrier toward nucleation resulting in crystallization at a faster rate than the normal crystallization rate (Li & Huneault, 2007). Several nucleating agents such as starch (Cai et al., 2011; Kang, Lee, Lee, Narayan, & Shin, 2008; Ke & Sun, 2003), talc (Haubruge, Daussin, Jonas, & Legras, 2003; Shakoor & Thomas, 2013; Yu et al., 2012), montmorillonite (Chu & Wu, 2007; Nam, Ray, & Okamoto, 2003), hydrazide compounds (Fan et al., 2013; Kawamoto, Sakai, Horikoshi, Urushihara, & Tobita, 2007), etc., have been reported.

Starch is a potential material for blending with PLA not only because it is completely biodegradability but there is also a natural abundance at a low cost. Starch is under strong inter- and intramolecular hydrogen bond networks; therefore, it is insoluble in most solvents and high hydrophilic. The processing of starch to be a plastic material is quite difficult due to degradation without melting at high temperature and the blending of starch with other polymers always faces the problem of phase separation. It is known that the modification of the hydroxyl groups on the anhydroglucose units (AGUs) with the hydrophobic group is a way to obtain compatibility with other polymers (Biswas, Shogren, Kim, & Willett, 2006; Kaur, Ariffin, Bhat, & Karim, 2012; Shogren, 2003; Zhou, Ren, Tong, Xie, & Liu, 2009). For PLA and starch blend in the past, the coupling agents to modify starch in order to form the covalent bonds with PLA such as methylenediphenyl diisocyanate (MDI) (Wang, Sun, & Seib, 2001, 2002a, 2002b), maleic anhydride (MA) (Xiong et al., 2013; Zhang & Sun, 2004b), dioctyl maleate (DOM) (Zhang & Sun, 2004a), etc., were also reported.

On this viewpoint, it comes to our idea that the blend of starch could be practical for the industries if we can modify starch to be reactive enough not only for coupling with the polymer but also for a one-pot reactive blend in processing machine.

Silane coupling agent is known for the function of combining two materials via the hydrolyzable and organofunctional reactive sides (Plueddemann, 1982). In the past, the uses of silane coupling agent for the reactive blend between starch and polymers were reported. For example, the compatibility between polyethylene and

starch (10 wt%) was successful when the starch was pre-treated with sodium alkyl siliconate (Griffin, 1994; Wu, Qi, Liang, & Zhang, 2006) demonstrated the improvement of interfacial adhesion between starch and rubber by using resorcinol-formaldehyde and N-β(aminoethyl)-aminopropyl trimethoxy silane.

In the case of PLA and silane treated starch blends, they were widely reported but mainly focused on the changes in mechanical and thermal properties (Liu, Cao, & Ou-Yang, 2013; Pilla, Gong, O'Neill, Rowell, & Krzysik, 2008). Although the use of silane coupling agent for starch and polymer was proven to be practical, the detailed structural analyses have not been completed.

Based on the above mentioned viewpoint, the present work pays an attention on the starch coupling with PLA via silane coupling agent in the reactive blend system. In the first step, a systematic study of coupling reaction between organofunctional silane coupling agents and starch to clarify the optimal type of silane was carried out. A detailed study on chemical structure by NMR technique led us to the qualitative and quantitative analyses for information of the bond formation as well as the degree of substitution of silane. In the second step, the use of the obtained starch coupling with silane for the reactive blend with PLA was focused. In this step, the studies related to (i) the detailed structural analysis to declare the coupling between silane modified starch (silane-starch) and PLA, (ii) the morphological studies to observe compatibility between starch and PLA, (iii) the thermal analysis to evaluate the effect of starch in the blend on the nucleation and the plasticity, and (iv) the tensile test to clarify the mechanical properties of the PLA blended with silane-starch were carried out.

3.3 Materials and Experimental

3.3.1 Materials

PLA 2002D was purchased from NatureWorks LLC, USA. Cassava starch was obtained from ETC International Trading Co., Ltd., Thailand. A series of trimethoxy silane coupling agents – 3-glycidoxypropyl trimethoxysilane (GPMS), 3-aminopropyl trimethoxysilane (APMS), and 3-chloropropyl trimethoxysilane

(CPMS) – were bought from Sigma-Aldrich, Germany, with 97–98% purity. All reagents were used without further purification.

3.3.2 Sample Preparations (Scheme 3.1)

3.3.2.1 Modification of Starch with GPMS, APMS, and CPMS

A trimethoxy silane coupling agent, GPMS (0.1 mol, 22.5 mL), was stirred vigorously with an excess amount of deionized water at 50 °C until the turbidity vanished before mixing with dry starch (1 mol, 162.0 g). The mixture was stirred thoroughly at 50 °C under vacuum for 2 h before filtrating and drying at 70 °C in a hot air oven for a day. The crude product was purified by washing twice with tetrahydrofuran (THF) before drying at 60 °C in a vacuum oven for 6 h to obtain GP-starch, **1**.

FTIR (KBr: υ, cm^{-1}) for GP-starch: 1210 (s, C–O stretching in epoxides), 1100–1000 (s, Si–O–CH_2 stretching), 1100–1000 (s, C–O–C stretching), and 850 (vs, Si–C stretching).

^{1}H-NMR (δ, ppm, 500 MHz, DMSO-d_6, 60 °C) for GP-starch: 1.20 (m, CH_2), 2.08 (s, CH_2), and 3.35 (br, CH) assigned to GPMS, and 3.35–3.85 (br, CH) and 4.73–5.15 (s, CH) assigned to AGUs.

The molar feed ratios between silanol and starch were varied from 0.01:1 to 1:1 to determine the optimal condition. Similarly, other silane coupling agents, APMS (0.1 mol, 17.9 mL) and CPMS (0.1 mol, 19.8 mL), were used to obtain AP-starch (the possible structures: **2** and/or **3**), and CP-starch (the possible structures: **4** and/or **5**), respectively.

FTIR (KBr; υ, cm^{-1}) for AP-starch: 1575 (br, NH bending), 1150 (s, Si–O–Si stretching), 1100–1000 (s, C–O–C stretching), and 850 (vs, Si–C stretching).

^{1}H-NMR (δ, ppm, 500 MHz, D_2O, 60 °C) for AP-starch: 0.58 (s, CH_2), 1.60 (s, CH_2), and 2.82 (s, CH_2) assigned to APMS, and 3.63–3.80 (br, CH), 3.90 (s, CH_2), and 5.15 (s, CH) assigned to AGUs.

FTIR (KBr; υ, cm^{-1}) for CP-starch: 1275 (s, CH_2–Cl wagging), 1100–1000 (s, Si–O–CH_2 stretching), 1100–1000 (s, C–O–C stretching), 890 (s, C–Cl stretching), and 850 (vs, Si–C stretching).

^{1}H-NMR (δ, ppm, 500 MHz, DMSO-d_6, 60 °C) for CP-starch: 0.8 (s, CH2), 1.85 (s, CH2), and 3.60 (br, CH2) assigned to CPMS, and 3.40–3.70 (br, CH) and 4.73–5.15 (s, CH) assigned to AGUs.

3.3.2.2 Blending of PLA with GP-starch, AP-starch, and CP-starch

GP-starch was blended with PLA resin at weight ratios (PLA/GP-starch) of 90/10, 70/30, and 50/50 by using a Labtech Engineering LTE 20-40 counter-rotating twin screw extruder. The temperature and screw speed settings were in the range of 150–165 °C and 25–40 rpm, respectively. The 90/10 blend was blown to obtain a PLA/GP-starch film with ~0.10 mm thickness by using a Labtech Engineering LE 20-30 single-screw extruder equipped with a Labtech Engineering LF-400 blown film unit. Other films, PLA/AP-starch and PLA/CP-starch, were prepared with similar procedures.

3.3.3 Characterizations

3.3.3.1 Structural Characterization

The detailed structural analyses were completed by using a Bruker Equinox 55/FRA106S Fourier transform infrared (FT-IR) spectrometer (a resolution of 2 cm^{-1} (32 scans), in the range of 4000–400 cm^{-1}), and a Bruker Biospin Avance 500 NMR (nuclear magnetic resonance) spectrometer (based on ^{1}H–^{1}H TOCSY (total correlation spectroscopy) NMR spectrum at 60 °C). Deuterated dimethyl sulfoxide (DMSO-d_6) was the NMR solvent for GP-starch, CP-starch, and their silanols while deuterium oxide (D_2O) was for AP-starch and APMS silanol. In the cases of PLA/silane-starch blends, the samples of the 50/50 weight ratio were used and dis- solved in deuterated chloroform ($CDCl_3$). The degree of substitution (DS) of silane on starch was calculated from ^{1}H-NMR spectra using Eq. (1):

$$DS = \frac{\text{integration of } (-CH_2-) \text{ at } 1.6\text{–}2.0 \text{ ppm}}{2 \times 3 \times \text{integration of } (-CH-) \text{ at } 5.0\text{–}5.3 \text{ ppm}} \quad (1)$$

where the integrations of ($-CH_2-$) at 1.6–2.0 ppm and ($-CH-$) at 5.0–5.3 ppm represent the methylene protons of silane and the methine proton of AGU, respectively.

3.3.3.2 Contact Angle Measurement

Starch, GP-starch, AP-starch, and CP-starch were pressed to form pellets before measuring the contact angle with a KRÜSS DSA 10 drop shape analysis system.

3.3.3.3 Thermal Analyses

Thermal analyses were evaluated by using a TA Instruments Q50 thermal gravimetric analyzer (TGA), in the range of 30–700 °C with a heating rate of 5 °C/min under nitrogen flow (10 mL/min), and a Netzsch 200 F3 Maia differential scanning calorimeter (DSC), the sample (10 mg) was sealed in an aluminum pan and heated from −20 °C to 200 °C (heat–cool–heat) with a heating and cooling rate of 5 °C/min under nitrogen flow (50 mL/min). The degree of crystallinity (X_c) of PLA was calculated from the second scan using Eq. (2):

$$X_c\,(\%) = (\Delta H_m,PLA \times 100)/(X_{PLA} \times \Delta H_m) \quad (2)$$

where ΔH_m,PLA is the observed enthalpy change of fusion of PLA and X_{PLA} is the PLA weight fraction in the blend. ΔH_m is 93.1 J/g for 100% crystalline PLA (Fischer, Sterzel, & Wegner, 1973).

3.3.3.4 Morphological Observation

The cross-section surface of PLA/silane-starch 90/10 blends were investigated by using a Hitachi TM-1000 scanning electron microscope (SEM). The samples were fractured in liquid nitrogen and sputter-coated with gold. The PLA/starch and PLA/CP-starch 90/10 blends were also observed by a Park Systems XE-100 atomic force microscope (AFM) under non-contact mode with a 910MACTA cantilever. The AFM measurement was operated at a scan speed of 0.4 Hz with a scan area of 5 × 5 m^2.

3.3.3.5 Mechanical Properties Characterization

The mechanical properties of the films were measured at 25 °C with a tensile load of 5 kN and a cross-head speed of 500 mm/min, according to ASTM D882 by using an Instron 4206 universal testing machine.

3.3.3.6 Statistical Analysis

The statistical analysis was performed by using SPSS (16.0) statistical software. The mean values of the experiments for crystallization and mechanical properties characterizations were determined by using one-way ANOVA at a level of significance 0.05 while Duncan post hoc multiple comparison test was applied to define the statistically significant differences among the groups.

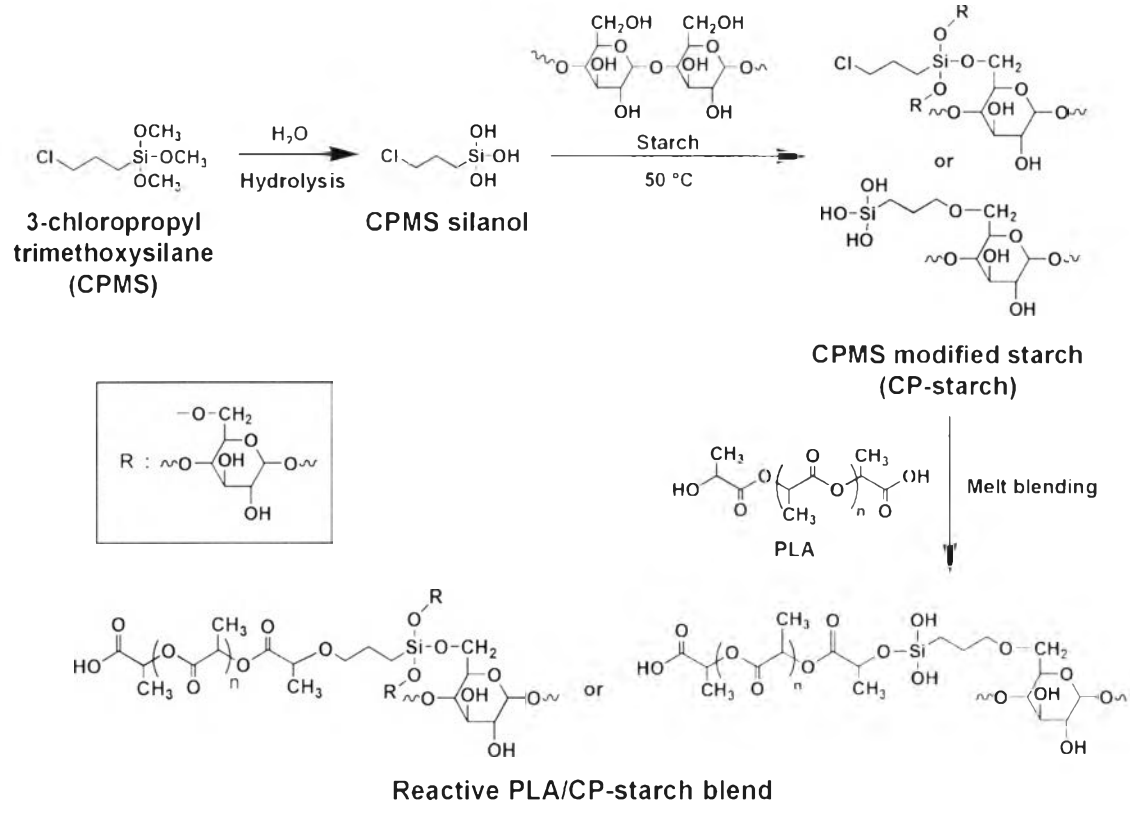

Scheme 3.1 Steps of starch coupling reaction with CPMS and melt blend.

3.4 Results and Discussion

3.4.1 Structural Characterization of Silane-starch

Three different organofunctional silane coupling agents, GPMS, APMS, and CPMS, were selected. The success of starch modification with various silane coupling agents was traced with FTIR spectra. In the case of GP-starch (Figure 3.1A(a)), the characteristic peaks at 915 cm^{-1} and 1210 cm^{-1} of the oxirane ring are observed. The characteristic peaks of the –Si–O–CH_2– group are in the range of 1150

cm^{-1} to 1050 cm^{-1} although it should be noted that these peaks partially overlap those of –C–O–C– stretching belonging to AGUs. For the AP-starch (Figure 3.1A(b)), the weak and broad peak at 1575 cm^{-1} referred to –NH– bending is identified. For the CP-starch (Figure 3.1A(c)), the strong C–Cl stretching and CH_2–Cl wagging peaks are at 890 cm^{-1} and 1275 cm^{-1}, respectively. This indicates that the coupling of each silane on the starch might occur via silanol linkages.

Quantitative ^{1}H-NMR analysis was applied to determine the degree of substitution (DS) of silane on AGUs. The DS was calculated according to Eq. (1) and all plotted in Figure 1B. All types of silane-starch show the maximum DS, 0.44 ± 0.02, 0.41 ± 0.01, and 0.24 ± 0.03 for GP-starch, AP-starch, and CP-starch, respectively, when the molar feed ratio of silanol:starch was 0.5:1. It should be noted that although the content of silanol was increased to a 1:1 molar feed ratio, the maximal DS was saturated at a specific feed ratio depending on the type of silane coupling agent.

^{1}H–^{1}H TOCSY NMR spectra were analyzed to identify the possible structures of starch modified with varied silane coupling agents (Figure 3.2). It has to be mentioned that all silane-starch were carefully dissolved in the NMR solvent although they were not completely soluble.

Figure 3.2a represents the case of GP-starch where a cross peak at 1.20 ppm (C**H**$_2$-I of GPMS) and at 3.98 ppm (C**H**$_2$-6 of AGU) is observed. It is important to note that the correlation between C**H**-V of GPMS at 3.35 ppm and C**H**-2 of AGU at 3.58 ppm indicates that the ring opening of the epoxy group formed the ether linkage between starch at the C-2 position and the oxirane ring. In other words, the GP-starch forms crosslink networks among AGUs. This implies the structure as shown in **1**.

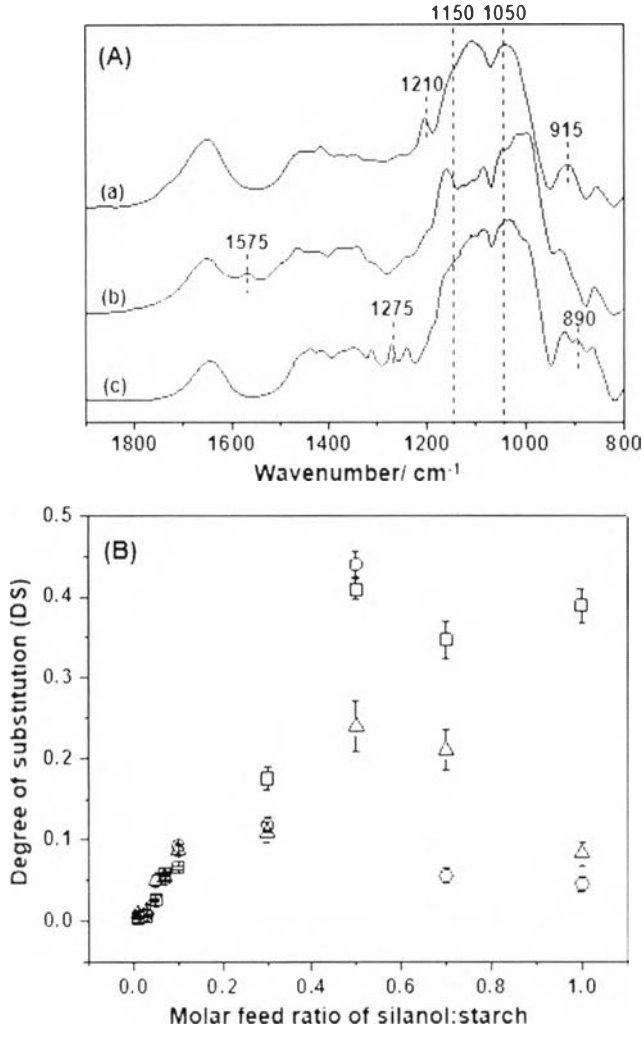

Figure 3.1 FTIR spectra (A) of GP-starch (a), AP-starch (b), and CP-starch (c), and degree of substitution of silane on starch (DS) (B) of GP-starch (○), AP-starch (□), and CP-starch (△) calculated following to Eq. (1).

For AP-starch (Figure 3.2b), the cross peak between C**H**$_2$-II of APMS at 1.65 ppm and C**H**-2 of AGU at 3.55 ppm exists together with the peak between C**H**$_2$-I of APMS at 1.25 ppm and C**H**$_2$-6 of AGU at 3.98 ppm. This correlation indicates the possible structures of AP-starch as **2** and **3**.

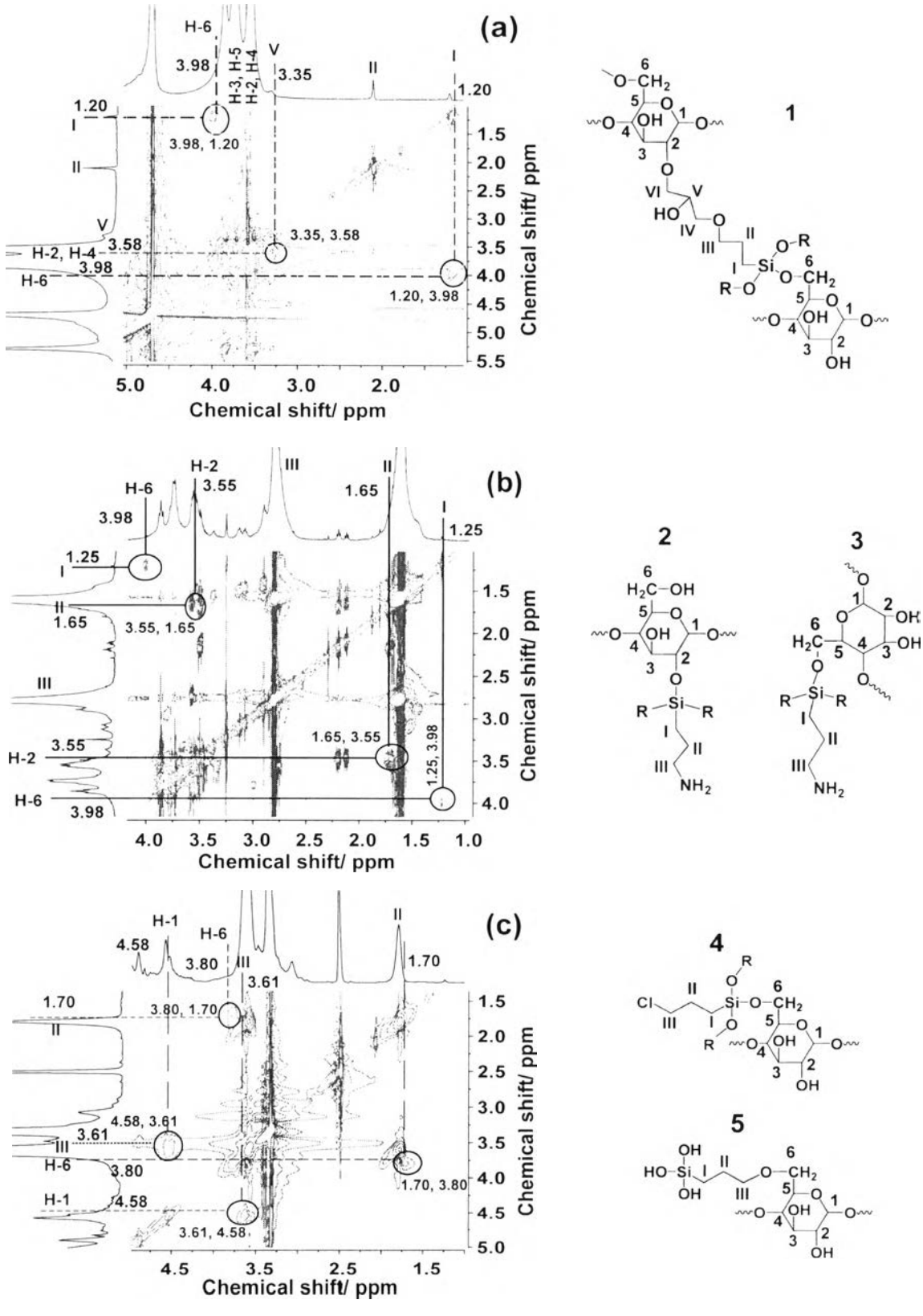

Figure 3.2 ^{1}H–^{1}H TOCSY NMR spectra of GP-starch in DMSO-d_6 (a), AP-starch in D_2O (b), and CP-starch in DMSO-d_6 (c).

In the case of CP-starch (Figure 3.2c), the spectrum suggests two possible structures, 4 and 5, the cross peaks represent the correlation between CH2-II of CPMS at 1.70 ppm and CH2-6 of AGU at 3.80 ppm, and between CH2-III of CPMS at 3.61 ppm and CH-1 of AGU at 4.58 ppm. From the possible structures 1 to 5, it could be concluded that both reactive groups, organofunctional and silanol groups, form the covalent bond with hydroxyl groups on AGUs.

However, the reactive blend between PLA and silane-starch is possible when the remaining functional groups on the silane-starch perform the reaction with hydroxyl and/or carboxylic groups of PLA chains in the melt blending step. Although CP-starch produces relatively low DS, as shown in Figure 3.1B, the remaining chloropropyl groups could effectively form the covalent bond with PLA through the hydroxyl and/or carboxylic groups.

3.4.2 Physico-chemical Properties of Silane-starch

The improved hydrophobicity of the starch after modification is preferable to obtain compatibility between PLA and starch. In this study, all samples were pressed into pellet form and the surface hydrophilicity was evaluated. Figure 3.3 shows that the water contact angle of the neat PLA is ~70° indicating relatively hydrophobic PLA. For starch, the water is quickly and completely absorbed (Figure 3.3b). Both GP-starch and AP-starch show the rapid water absorption while CP-starch shows the retained water droplet with the contact angle as high as 60°. This suggests not only the hydrophobicity improvement of starch by CPMS but also the possibility that CP-starch is compatible with PLA. The results also reflect that the different types of silane coupling agents bring in the different coupling structures. In the case of the GP-starch, the correlation in ^{1}H–^{1}H TOCSY NMR spectrum suggested the crosslink among AGUs. This led to an increase of hydroxyl groups along the GP-starch structure and as a result, GP-starch shows the significant hydrophilicity. For the AP-starch, as shown in the proposed structures (**2** and/or **3** (Figure 3.2b), the amine group of APMS could be the functional group to enhance the water absorption. Contrary to the CP-starch, as shown in **4** of Figure 3.2c, the hydrophobic chloropropyl group might be the key factor to induce the hydrophobicity.

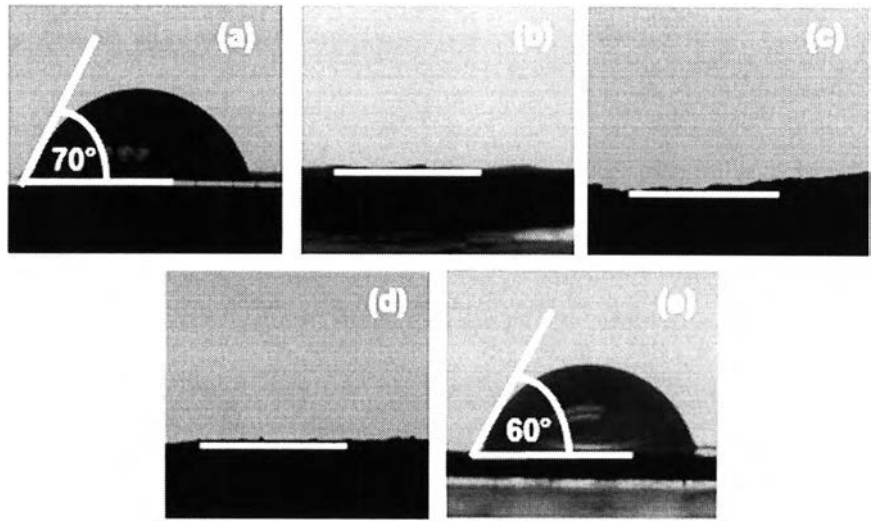

Figure 3.3 Water contact angle of PLA film (a), starch (b), GP-starch (c), AP-starch (d), and CP-starch (e).

The intra- and intermolecular hydrogen bonds in starch are very robust leading to the degradation before melting (Jenkins & Donald, 1995; Mani & Bhattacharya, 1998). Here, the starch shows an onset degradation temperature (T_d onset) of 287°C (Figure 3.4A(a)) while the GP-starch with the maximal DS (0.44) performs two T_d onset at 287 °C and 384 °C (Figure 3.4A(b)). The high T_d onset at 384 °C implies the partial crosslink network of AGUs by GPMS as in **1** of (Figure 3.2a). The structures proposed in **2**–**5** (Figure 3.2) lead to the weakening of their hydrogen bond networks, and as a consequence, the T_d decreases. As expected, AP-starch and CP-starch with maximal DS (0.41 and 0.24, respectively) show T_d onset at 279 °C and 255 °C, accordingly (Figure 3.4A(c) and (d)). This implies that the intermolecular hydrogen bonds between starch molecules were obstructed after modifying starch with APMS and CPMS. Consequently, it influenced the packing structures of silane-starch (see packing structures of silane-starch session). In fact, the residues, after degradation of all silane-starch, are around 20–35% (Figure 3.4A(b)–(d)), which are higher than that of starch (~12%). This suggests a crosslink network formation via silanol bonds among the starch chains.

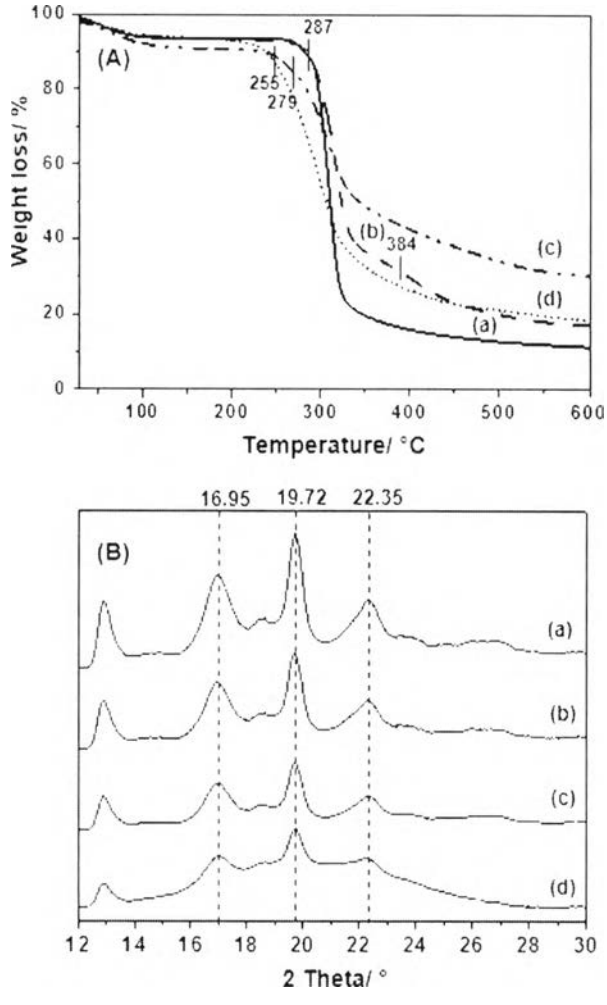

Figure 3.4 TGA thermograms (A) and WAXD patterns (B) of starch (a), GP-starch (b), AP-starch (c), and CP-starch (d).

WAXD pattern is a good tool used to trace the change in packing structures of starch after coupling with silane. Starch performs a typical C-type crystalline structure (Jang, Shin, Lee, & Narayan, 2007) of which the diffraction peaks at 16.95° 2θ, 19.72° 2θ, and 22.35° 2θ are clearly observed (Figure 3.4B(a)). GP-starch and AP-starch show the broad diffraction peaks (Figure 3.4B(b) and (c)) implying the loose packing structure. It should be noted that the peaks at 16.95° 2θ and 22.35° 2θ are almost disappeared when starch was treated with CPMS (Figure 3.4B(d)). The loose packing could be a result from the weakening of the intermolecular hydrogen bonds between starch molecules. This suggests the successful coupling reaction of silane on starch.

3.4.3 Characterizations of PLA/Silane-starch Blends

3.4.3.1 Morphology of PLA/Silane-starch Blends

After the starch was treated with various silane coupling agents, the silane-starch with maximal DS were blended with PLA at different weight ratios (90/10, 70/30, and 50/50 PLA/silane-starch) by using a twin screw extruder. The reactive organofunctional and silanol groups on silane-starch were expected to form the covalent bond with PLA and consequently to give the compatibility.

After blending, the cross-section surface of each compound was observed by SEM. Figure 3.5A shows the morphology of the starch and PLA for the PLA/starch and PLA/silane-starch 10 wt% blends. It is clear that the PLA blends with starch (Figure 3.5A(a)), with GP-starch (Figure 3.5A(b)), and with AP-starch (Figure 3.5A(c)), show the starch granules with large gaps in PLA matrices. In the case of PLA/CP-starch blend (Figure 3.5A(d)), the CP-starch granules are almost completely surrounded by PLA matrix.

AFM in non-contact mode was further applied to confirm compatibility between PLA and CP-starch. In the case of PLA/starch blend, the starch particle in PLA matrices (Figure 3.5B(a)) is obviously observed and the surface height – at a distance 3–5 μm (x-axis in Figure 3.5C(a)) – was below zero degree (a negative signal). This confirms phase separation between PLA and the starch granules. In the case of PLA/CP-starch blend (Figure 3.5B(b) and C(b)), the rough surface with a small surface height variation, and without discontinuous phase region of CP-starch and PLA matrix, suggests compatibility. It has to be noted that the zero degree – at a distance 1 μm – occurred because the tip of the cantilever detected the edge of CP-starch particles on PLA matrix (Figure 3.5C(b)).

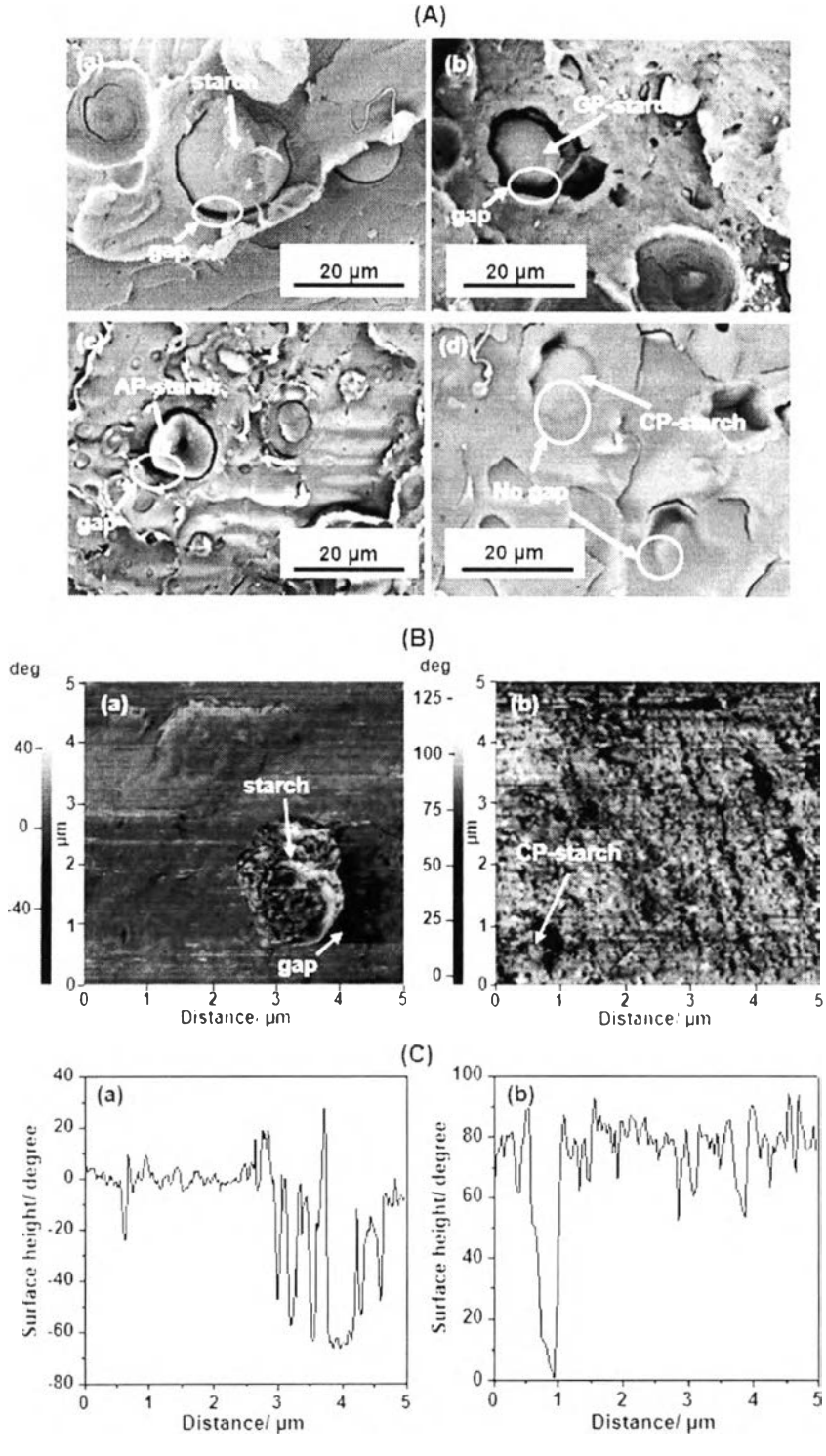

Figure 3.5 SEM micrographs (A) of PLA blended with 10 wt% starch (a), GP-starch (b), AP-starch (c), and CP-starch (d). AFM micrographs (B), and surface height (C) of PLA/starch (a) and PLA/CP-starch (b).

3.4.3.2 Crystallization of PLA/Silane-starch Blends

The neat PLA exhibits the glass transition temperature (T_g) at 56 °C, crystallization temperature (T_c) at 122°C, and melting temperature (T_m) at 154°C. The degree of crystallinity (X_c) was found to be ~4% (the Supporting information, Figure S1) (Martin & Avérous, 2001; Saeidlou, Huneault, Li, & Park, 2012). In previous research, starch was reported as a nucleating agent for low-density polyethylene (LDPE) (Ning, Jiugao, Xiaofei, & Ying, 2007), poly(hydroxyl ester ether) (PHEE) (Walia, Lawton, Shogren, & Felker, 2000), and polycaprolactone (PCL) (Kim, Kim, & Kim, 2007).

Here, in order to verify the starch as a nucleating agent of PLA, the crystallization behavior under non-isothermal condition was studied (Table 3.1). The second DSC scans of the samples obtained from all blending types and weight ratios were traced. One-way ANOVA and Duncan's multiple-range test were carried out to compare and differentiate the means of T_g, T_c, T_m, and X_c of the PLA/silane-starch blends. The T_g of PLA/GP-starch and PLA/APstarch blends was at ~60 °C. However, the T_g for all PLA/CP-starch blends, were found to be at ~50 °C. Although it is a small decrease, the result suggests that covalent bonds between CP-starch and PLA did obstruct the chain packing, or in other words, allow chain mobility.

The decrease in Tc reflects the effectiveness of nucleation. In this study, the T_c of PLA/AP-starch and PLA/CP-starch blends were found to be lower than that of the neat PLA for 10–15 °C (Table 3.1).

The X_c of PLA after blending was determined to observe the change in the crystalline phase. The PLA/CP-starch 90/10 blend which presents the good compatibility as in Figure 3.5A(d), shows the X_c of 30% which is 10 times higher than that of the neat PLA and 2 times higher than that of the PLA/starch 90/10 (Table 3.1). When the CP-starch content was increased to 30 wt%, it shows the X_c value of 53%, which was much higher than those of the PLA/starch, PLA/GP-starch, and PLA/AP-starch blends. This confirms that CP-starch induced crystallization of PLA.

It has been reported by Jang et al. (2007) that the X_c of PLA/starch treated with MA70/30 blend increased to 36%. This is in agreement with our finding of CP-starch as the nucleating agent.

Table 3.1 Thermal properties of PLA/silane-starch blends

Sample	Weight ratio	T_g (°C)	T_c (°C)	T_m (°C)	X_c (%)
Neat PLA	100/0	56.56 ± 1.24^{b}	122.81 ± 2.46^{ef}	154.27 ± 1.68^{cd}	4.75 ± 0.81^{a}
PLA/starch	90/10	56.77 ± 1.20^{b}	111.32 ± 1.11^{ab}	151.78 ± 1.53^{abc}	15.79 ± 0.75^{b}
PLA/GP-starch	90/10	60.49 ± 1.19^{e}	125.94 ± 4.01^{f}	151.05 ± 1.44^{abc}	16.21 ± 0.95^{b}
PLA/AP-starch	90/10	57.90 ± 0.81^{bcd}	117.76 ± 4.49^{cde}	152.23 ± 2.27^{abc}	28.88 ± 1.92^{d}
PLA/CP-starch	90/10	50.83 ± 1.54^{a}	113.72 ± 3.71^{abcd}	149.16 ± 0.96^{a}	30.86 ± 0.72^{de}
PLA/starch	70/30	57.55 ± 1.15^{bc}	113.43 ± 3.26^{abcd}	152.56 ± 2.49^{bc}	24.36 ± 1.29^{c}
PLA/GP-starch	70/30	59.49 ± 0.70^{de}	123.66 ± 4.70^{ef}	153.05 ± 1.98^{bcd}	23.27 ± 2.70^{c}
PLA/AP-starch	70/30	59.39 ± 1.10^{cde}	116.09 ± 3.19^{bcd}	155.82 ± 2.03^{d}	36.89 ± 1.86^{f}
PLA/CP-starch	70/30	51.18 ± 0.70^{a}	112.25 ± 1.90^{abc}	149.89 ± 1.15^{ab}	52.66 ± 1.00^{h}
PLA/starch	50/50	60.18 ± 0.53^{e}	119.03 ± 2.67^{de}	154.23 ± 1.41^{cd}	43.33 ± 2.32^{g}
PLA/GP-starch	50/50	57.88 ± 1.18^{bcd}	122.35 ± 3.68^{ef}	150.57 ± 0.98^{ab}	31.91 ± 2.26^{e}
PLA/AP-starch	50/50	59.68 ± 0.71^{de}	109.75 ± 1.47^{a}	154.20 ± 1.36^{cd}	37.97 ± 2.03^{f}
PLA/CP-starch	50/50	50.61 ± 0.79^{a}	115.12 ± 2.23^{abcd}	151.15 ± 1.45^{abc}	41.65 ± 1.16^{g}

*silane-starch at maximal DS

**Different letters denote statistically significant difference among the films at $p = 0.05$.

3.4.3.3 Mechanical Properties of PLA/Silane-starch Blends

After blending PLA with silane-starch, the compounds obtained were blown to be films. The selected content of starch and silane-starch in the blends for the blown films was 10 wt%. The mechanical properties, in terms of Young's modulus (E), tensile strength (TS), and elongation at break of all types of the films were identified (Table 3.2). One-way ANOVA and Duncan's multiple-range test were applied for statistical analysis. It was found that the E values of PLA after blending with starch and with silane-starch were ~2 GPa, however, the PLA/starch, PLA/GP-starch, and PLA/AP-starch films perform the slightly statistically different E values and are lower than that of PLA/CP-starch film. This reflects the phase separation of starch particles in PLA matrices (Figure 3.5A(a)–(c)).

In the past, several reports of PLA/starch blends (Wang, Sun, & Seib, 2001; Xiong et al., 2013; Zhang & Sun, 2004b) showed that *TS* significantly decreased due to phase separation between PLA and starch in the blend. Here, the similar results were also observed. The PLA/starch, PLA/GP-starch, and PLA/AP-starch films show the decreases in *TS* values (~20 MPa) (Table 3.2). In contrast, only the PLA/CP-starch film, has relatively high *TS* (~40 MPa) similar to the neat PLA film (*E*~2.2 GPa and *TS*~35 MPa). This also confirms that enhanced compatibility in the PLA/CP-starch film contributes to higher *E* and *TS* values.

Table 3.2 Mechanical properties of PLA/silane-starch 90/10 blends

Sample	Young's Modulus (*E*)/ GPa	Tensile strength (*TS*)/ MPa	Elongation at break/ %
Neat PLA	2.18 ± 0.23^{bc}	34.62 ± 3.43^{c}	2.10 ± 0.33^{b}
PLA/starch	1.91 ± 0.17^{a}	23.94 ± 3.97^{b}	2.04 ± 0.35^{b}
PLA/GP-starch	1.78 ± 0.15^{a}	19.56 ± 1.76^{a}	1.40 ± 0.19^{a}
PLA/AP-starch	1.95 ± 0.21^{ab}	21.57 ± 2.22^{ab}	1.32 ± 0.23^{a}
PLA/CP-starch	2.27 ± 0.21^{c}	39.40 ± 2.34^{d}	2.49 ± 0.32^{c}

*silane-starch at maximal DS
**Different letters denote statistically significant difference among the films at $p = 0.05$.

In the case of elongation at break, it should be noted that PLA/CP-starch film shows 2.5% which is slightly higher than those of the neat PLA and PLA/starch films (~2.3%), whereas the other PLA/GP-starch and PLA/AP-starch films show a significant decrease in elongation at break. It is known that starch is a highly crystalline polymer; therefore, the increase in elongation at break is not significant. In other words, the elongation at break of the PLA/CP-starch film is maintained as that of PLA film which reflects a good performance of CP-starch.

3.4.4 Structural Investigation of PLA/Silane-starch Blends

As the results suggested that the CP-starch initiates compatibility between PLA and starch via the reactive blend process, it is important to identify the chemical structure in details. Although the solubility of PLA/silane-starch blends in $CDCl_3$ was not quite completed, ^1H–^1H TOCSY NMR was applied to investigate the coupling of silane-starch and PLA.

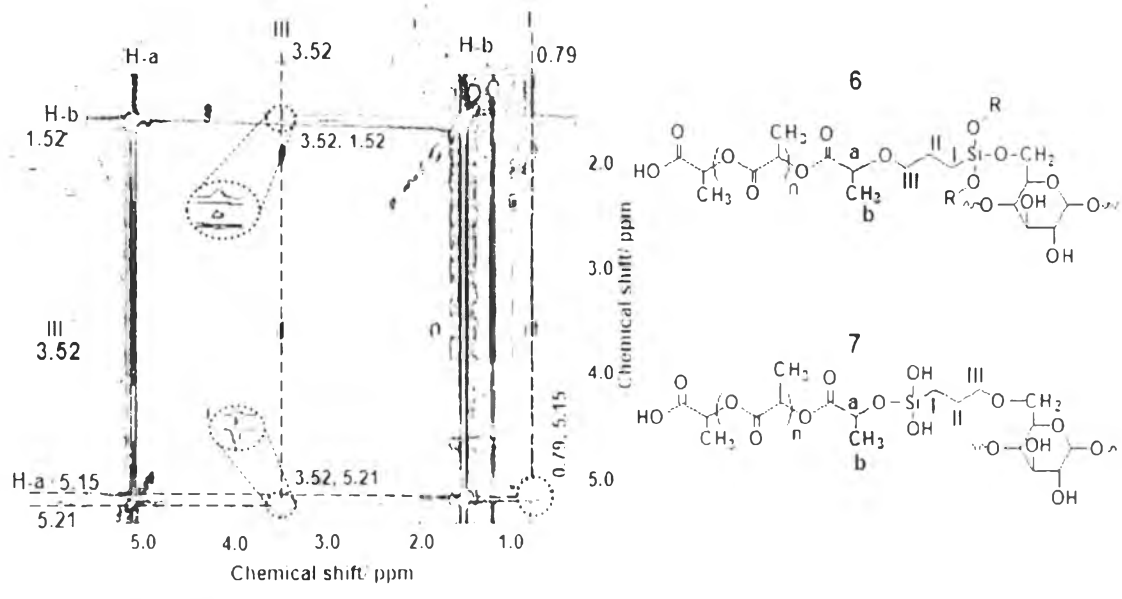

Figure 3.6 ^1H–^1H TOCSY NMR spectrum of the reactive PLA/CP-starch blend.

For PLA/starch 50/50 blend, there was no correlation in ^1H–^1H TOCSY NMR spectrum between PLA chain and starch molecule (the Supporting information, Figure S2). In fact, neither PLA/GP-starch nor PLA/AP-starch blend showed the correlations indicating that there was no covalent bond between PLA and GP-starch or AP-starch (the Supporting information Figures S3 and S4). In other words, the blends of PLA and starch treated with GPMS and/or APMS were incompatible. For the PLA/CP-starch blend, the correlation between PLA and CP-starch is observed through ^1H–^1H TOCSY NMR spectrum as shown in Figure 3.6. The signals designated as H-a at 5.21 ppm and as H-b at 1.52 ppm are attributed to –CH– and $-CH_3$ protons of PLA chains, respectively. The two cross peaks, i.e. the one at between 1.52 ppm (H-b) and/or 5.21 ppm (H-a) and 3.52 ppm ($-CH_2$-III) and the other peak at between 5.15 ppm (H-a) and 0.79 ppm ($-CH_2$-I), are observed

evidently. The results suggest the possible structures shown in 6 and 7 (Figure 3.6). It should be noted that the compatibility in PLA/CP-starch blend was successful due to the covalent bonds formation between PLA chain and CP-starch molecule.

3.5 Conclusions

The present work proposed the reactive blend between starch and PLA to obtain the compatible blend. Silane coupling agents, GPMS, APMS, and CPMS, performed the successful coupling with starch to form GP-starch, AP-starch, and CP-starch with the degree of substitution in the range of 0.2–0.5 depending on the type of silane coupling agent as identified by FTIR, and TOCSY NMR. The TOCSY NMR spectra indicated that only CP-starch formed the covalent bonds with PLA to produce the reactive blend. The reactive PLA/CP-starch 90/10 blend showed a decrease in T_g for almost 10 °C and a 10-fold increase of degree of crystallinity. SEM and AFM micrographs established that PLA and CP-starch were compatible. The PLA/CP-starch film had comparative mechanical properties to PLA, with relatively high tensile strength.

3.6 Acknowledgements

The authors wish to thank the Thailand Research Fund (the Royal Golden Jubilee Ph.D. scholarship program PHD/0188/2550 and TRF-OSMEP research grant) for financial support as well as the Center for Petroleum, Petrochemical, and Advanced Materials, Chulalongkorn University, Thai Plastic Bags Co., Ltd.; and Wandee Plastic Agencies Co., Ltd for the research facilities.

3.7 References

Biswas, A., Shogren, R. L., Kim, S., & Willett, J. L. (2006). Rapid preparation of starch maleate half-esters. *Carbohydrate Polymers*, 64(3), 484–487.

Cai, J., Liu, M., Wang, L., Yao, K., Li, S., & Xiong, H. (2011). Isothermal crystallization kinetics of thermoplastic starch/poly(lactic acid) composites. *Carbohydrate Polymers*, 86(2), 941–947.

Chu, M.-J., & Wu, T.-M. (2007). Isothermal crystallization kinetics of poly(lactic acid)/montmorillonite nanocomposites. In E. E. Gdoutos (Ed.), Experimental analysis of nano and engineering materials and structures (pp. 827–828). Dordrecht, The Netherlands: Springer.

Fan, Y., Yu, Z., Cai, Y., Hu, D., Yan, S., Chen, X., & Yin, J. (2013). Crystallization behavior and crystallite morphology control of poly(l-lactic acid) through N,N′-bis(benzoyl)sebacic acid dihydrazide. *Polymer International*, 62(4), 647–657.

Fischer, E. W., Sterzel, H., & Wegner, G. (1973). Investigation of the structure of solution grown crystals of lactide copolymers by means of chemical reactions. *Kolloid-Zeitschrift und Zeitschrift für Polymere*, 251(11), 980–990.

Garlotta, D. (2002). A literature review of poly(lactic acid). *Journal of Polymers and the Environment*, 9(2), 63–84.

Griffin, G. J. L. (Ed.). (1994). Chemistry and technology of biodegradable polymers. Glasgow: Chapman and Hall.

Haubruge, H. G., Daussin, R., Jonas, A. M., & Legras, R. (2003). Epitaxial nucleation of poly(ethylene terephthalate) by talc: Structure at the lattice and lamellar scales. *Macromolecules*, 36(12), 4452–4456.

Huneault, M. A., & Li, H. (2007). Morphology and properties of compatibilized polylactide/thermoplastic starch blends. *Polymer*, 48(1), 270–280.

Jang, W. Y., Shin, B. Y., Lee, T. J., & Narayan, R. (2007). Thermal properties and morphology of biodegradable PLA/starch compatibilized blends. *Journal of Industrial and Engineering Chemistry*, 13(3), 457–464.

Jenkins, P. J., & Donald, A. M. (1995). The influence of amylose on starch granule structure. *International Journal of Biological Macromolecules*, 17(6), 315–321.

Kang, K., Lee, S., Lee, T., Narayan, R., & Shin, B. (2008). Effect of biobased and biodegradable nucleating agent on the isothermal crystallization of poly(lactic acid). *Korean Journal of Chemical Engineering*, 25(3), 599–608.

Kaur, B., Ariffin, F., Bhat, R., & Karim, A. A. (2012). Progress in starch modification in the last decade. *Food Hydrocolloids*, 26(2), 398–404.

Kawamoto, N., Sakai, A., Horikoshi, T., Urushihara, T., & Tobita, E. (2007). Nucleating agent for poly(l-lactic acid)—An optimization of chemical structure of hydrazide compound for advanced nucleation ability. *Journal of Applied Polymer Science*, 103(1), 198–203.

Ke, T., & Sun, X. (2003). Melting behavior and crystallization kinetics of starch and poly(lactic acid) composites. *Journal of Applied Polymer Science*, 89(5), 1203–1210.

Kim, E. G., Kim, B. S., & Kim, D. S. (2007). Physical properties and morphology of polycaprolactone/starch/pine-leaf composites. *Journal of Applied Polymer Science*, 103(2), 928–934.

Li, H., & Huneault, M. A. (2007). Effect of nucleation and plasticization on the crystallization. *Polymer*, 48(23), 6855–6866.

Liu, R., Cao, J., & Ou-Yang, L. (2013). Degradation of wood flour/poly(lactic acid) composites reinforced by coupling agents and organo-montmorillonite in a compost test. *Wood and Fiber Science*, 45(1), 105–118.

Mani, R., & Bhattacharya, M. (1998). Properties of injection moulded starch/synthetic polymer blends—IV. Thermal and morphological properties. *European Polymer Journal*, 34(10), 1477–1487.

Martin, O., & Avérous, L. (2001). Poly(lactic acid): Plasticization and properties of biodegradable multiphase systems. *Polymer*, 42(14), 6209–6219.

Nam, J. Y., Ray, S. S., & Okamoto, M. (2003). Crystallization behavior and morphology of biodegradable polylactide/layered silicate nanocomposite. *Macromolecules*, 36(19), 7126–7131.

Ning, W., Jiugao, Y., Xiaofei, M., & Ying, W. (2007). The influence of citric acid on the properties of thermoplastic starch/linear low-density polyethylene blends. *Carbohydrate Polymers*, 67(3), 446–453.

Pilla, S., Gong, S., O'Neill, E., Rowell, R. M., & Krzysik, A. M. (2008). Polylactide-pine wood flour composites. *Polymer Engineering and Science*, 48(3), 578–587.

Plueddemann, E. P. (Ed.). (1982). Silane coupling agents. New York, NY: Plenum Press.

Saeidlou, S., Huneault, M. A., Li, H., & Park, C. B. (2012). Poly(lactic acid) crystallization. *Progress in Polymer Science*, 37(12), 1657–1677.

Shakoor, A., & Thomas, N. L. (2013). Talc as a nucleating agent and reinforcing filler in poly(lactic acid) composites. *Polymer Engineering and Science*, 54(1), 64–70.

Shogren, R. L. (2003). Rapid preparation of starch esters by high temperature/pressure reaction. *Carbohydrate Polymers*, 52(3), 319–326.

Walia, P. S., Lawton, J. W., Shogren, R. L., & Felker, F. C. (2000). Effect of moisture level on the morphology and melt flow behavior of thermoplastic starch/poly(hydroxy ester ether) blends. *Polymer*, 41(22), 8083–8093.

Wang, H., Sun, X., & Seib, P. (2001). Strengthening blends of poly(lactic acid) and starch with methylenediphenyl diisocyanate. *Journal of Applied Polymer Science*, 82(7), 1761–1767.

Wang, H., Sun, X.,&Seib, P. (2002a). Effects of starch moisture on properties of wheat starch/poly(lactic acid) blend containing methylenediphenyl diisocyanate. *Journal of Polymers and the Environment*, 10(4), 133–138.

Wang, H., Sun, X., & Seib, P. (2002b). Mechanical properties of poly(lactic acid) and wheat starch blends with methylenediphenyl diisocyanate. *Journal of Applied Polymer Science*, 84(6), 1257–1262.

Wu, Y.-P., Qi, Q., Liang, G.-H., & Zhang, L.-Q. (2006). A strategy to prepare high performance starch/rubber composites: In situ modification during latex compounding process. *Carbohydrate Polymers*, 65(1), 109–113.

Xiong, Z., Li, C., Ma, S., Feng, J., Yang, Y., Zhang, R., & Zhu, J. (2013). The properties of poly(lactic acid)/starch blends with a functionalized plant oil: Tung oil anhydride. *Carbohydrate Polymers*, 95(1), 77–84.

Yu, F., Liu, T., Zhao, X., Yu, X., Lu, A., & Wang, J. (2012). Effects of talc on the mechanical and thermal properties of polylactide. *Journal of Applied Polymer Science*, 125(S2), E99–E109.

Zhang, J.-F., & Sun, X. (2004a). Mechanical and thermal properties of poly(lactic acid)/starch blends with dioctyl maleate. *Journal of Applied Polymer Science*, 94(4), 1697–1704.

Zhang, J.-F., & Sun, X. (2004b). Mechanical properties of poly(lactic acid)/starch composites compatibilized by maleic anhydride. *Biomacromolecules*, 5(4), 1446–1451.

Zhou, J., Ren, L., Tong, J., Xie, L., & Liu, Z. (2009). Surface esterification of corn starch films: Reaction with dodecenyl succinic anhydride. *Carbohydrate Polymers*, 78(4), 888–893.